Poly(Ethylene Oxide)/Organosolv Lignin Blends: Relationship between Thermal Properties, Chemical Structure, and Blend Behavior

Satoshi Kubo and John F. Kadla*

Biomaterials Chemistry, Faculty of Forestry, University of British Columbia, Vancouver, B.C., V6T 1Z4 Canada

Received May 13, 2004; Revised Manuscript Received June 13, 2004

ABSTRACT: Blends of poly(ethylene oxide) with organosolv lignin (Alcell) were prepared by thermal blending. Excellent fiber spinning was achieved over the entire blend ratio. The good thermal properties of the Alcell lignin arise from its unique chemical structure. HMQC 2D NMR analysis revealed the presence of alkoxyl chains at the Cα and Cγ positions of the Alcell lignin side chain structure acting as internal plasticizers and enhancing the thermal mobility of the lignin. The addition of a small amount of Alcell lignin to PEO resulted in an increase of the PEO crystalline domain size. However, both PEO crystallinity and crystalline domain size decreased with lignin incorporation beyond 25 wt %. A negative polymer−polymer interaction energy density "*B*" was calculated on the basis of the melting point depression of PEO and a negative deviation of T_g from the weighted average values observed. Good prediction of the T_g-composition behavior was obtained indicating the presence of favorable interactions between blend components. FT-IR analysis revealed the formation of a strong hydrogen-bonding system between Alcell lignin and PEO, supporting that hydrogen-bonding interactions are an important factor in the formation of miscible lignin-based polymer blends.

Introduction

The utilization of lignins in biodegradable/biobased materials is receiving increasing attention as the world looks to find alternatives to petrochemicals.[1] Traditionally, lignins have been incorporated into various polymeric materials as low cost filler. In such systems, the amount of lignin being introduced is maximized to a level where minimal loss of mechanical properties occurs. Lignin is extremely promising in its ability to facilitate the biodegradation of polyolefins.[2] Thermoplastics with very high lignin content have been produced by alkylating kraft lignin[3] or blending kraft lignin with synthetic polymers.[4−7] These new lignin-based materials possess tensile behavior comparable to polystyrene. Although 100% kraft lignin and alkylated kraft lignin films and fibers are quite brittle, they can be effectively plasticized by blending with suitable polyesters[5,7] and polyethers.[4] For example, by incorporating 5% poly(ethylene oxide) into hardwood kraft lignin continuous fibers can be spun and exhibit a nearly 10% increase in tensile strength and Young's modulus.[4]

Lignin is one of the most abundant biomacromolecules. It exists in plant cell walls and is second only to cellulose in overall natural abundance. Enormous amounts of industrial lignin are produced as byproducts of papermaking.[8] Despite this, the utilization of lignin is still constrained. Lignin biosynthesis, which involves dehydrogenative radical coupling of monolignols, results in a highly cross-linked three-dimensional structure.[9−11] Technical lignins, such as kraft lignins and organosolv lignins (lignins extracted from wood chips through chemical treatment with aqueous sodium hydroxide/sodium sulfide or acidic ethanol, respectively) have undergone extensive depolymerization and chemical changes. Depending on the type and length of chemical processing, the lignins will vary in molecular weight, functional groups present, degree of condensation, types of intermonomeric linkages, and the type and ratio of monomeric units. Pronounced noncovalent attractive interactions also exist between individual molecular lignin species resulting in enormous associated complexes.[12,13] These supramacromolecular complexes are responsible for the cohesive nature of lignin-based materials.[7]

Recently, we have demonstrated that hardwood kraft lignin form miscible blends with poly(ethylene oxide).[4] It was found that phenolic hydroxyl groups form stronger hydrogen bonds with the ether oxygen in poly(ethylene oxide) than aliphatic hydroxyl groups. Moreover, the hydrogen bonds formed between lignin and poly(ethylene oxide) are significantly stronger than those within the lignin macromolecule itself. The glass-transition temperature (T_g) showed a negative deviation from a linear mixing rule suggesting a polymer blend system involving weak specific intermolecular interactions.

Organosolv lignins differ significantly from other technical lignins. Structurally, organosolv lignins have a higher relative amount of phenolic hydroxyl groups, a more oxidized structure (Hibbert's ketones), possess low T_g's, and are easier to thermally process than kraft lignins. As a result, organosolv lignins have advantages over other industrial lignins for composite-material applications. We have shown that Alcell (organosolv lignin isolated by acidic ethanolysis of hardwood) is readily transformed into filament form suitable for carbon fibers without any chemical modification.[14] Feldman et al.[15] reported that Alcell/poly(vinyl chloride) composites possess superior mechanical properties over comparable kraft and sodium lignosulfonate-based materials. Although many reports exist documenting organosolv lignin structure related to pulping and bleaching chemistry,[16] few papers discuss the relationship

* Corresponding author. Address: 4034 Forest Science Centre, Department of Wood Science, The University of British Columbia, Vancouver, B.C., V6T 1Z4 Canada; telephone: +1-604-857-5254; fax: +1-604-822-9104; e-mail: john.kadla@ubc.ca.

10.1021/ma0490552 CCC: $27.50
Published on Web 07/31/2004

between chemical structure and moldability, the thermal properties of organosolv lignins, and their corresponding polyblends. In this study, the effect of Alcell chemical structure on the thermal properties of Alcell and blends with poly(ethylene oxide) are discussed and compared to those previously reported for hardwood kraft lignins.

Experimental Section

Materials. Alcell (Repap Enterprises Inc.) and poly(ethylene oxide) (PEO), 100 000 amu (Union Carbide Corp.) were used as received. All solvents and chemicals were purchased from Aldrich Chemicals and used as received.

Lignin Characterization. Methoxyl content was determined according to the modified procedure of Viebock and Schwappach.[17] Syringyl/guaiacyl ratio was estimated using the nitrobenzene oxidation method.[18] Aliphatic and aromatic hydroxyl contents were determined using ^{1}H NMR.[19] Quantification was obtained from the integration ratios of aliphatic and aromatic acetoxy protons of acetylated lignin preparations relative to the internal standard, *p*-nitrobenzaldehyde.

The lignin preparations were acetylated by dissolving 200 mg of the lignin in 10 mL of pyridine:acetic anhydride (1:1, v/v) and stirring for 48 h at room temperature. The solution was poured over crushed ice and filtered. The resulting precipitate was then washed with cold water/HCl, dried, and subjected to a second acetylation treatment.

The relative average molecular mass and molecular mass distribution of acetylated lignin samples were determined by GPC (Waters Associates, UV and RI detectors) using styragel columns at 50 °C and THF as the eluting solvent. The GPC system was calibrated by using standard polystyrene samples. The injection volume was 100 μL, and the acetylated lignin concentration was 1 mg mL^{-1} in THF.

^{1}H−^{13}C Correlation 2D NMR Spectroscopy. Spectra were recorded on a Bruker AVANCE 500 MHz spectrometer (1996) using an Oxford narrow bore magnet (1989) in DMSO-d_6; the DMSO-d_6 cross-peak at δ_C/δ_H 39.5/ 2.5 was used as an internal reference. Forty milligrams of dry lignin were accurately weighed and dissolved in 0.75 mL of DMSO-d_6. The system was controlled by the SGI INDY host workstation and the data was processed with XWIN NMR. The instrument was equipped with three frequency channels, waveform memory, and amplitude shaping and three-channel gradient control units (GRASP III) and one variable temperature unit, as well as one unit for precooling and temperature stabilization. All measurements were carried out with a 5-mm ID ^{1}H/BB (^{109}Ag−^{31}P) triple-axis gradient probe (ID500−5EB, Nalorac Cryogenic Corp.). The operational frequency for ^{1}H nucleus was 500.128 MHz and conditions for analysis included a 90° pulse width of 10 μs and a 1.5-μs pulse delay (d_1).

Blend Preparation. Alcell was thermally treated at 160 °C under vacuum for 30 min to remove volatile contaminants. Blends of various Alcell/lignin ratios were prepared by mechanical mixing followed by thermal extrusion using an Atlas Laboratory Mixing Extruder (Atlas Corp.) equipped with 1/32 in. (ca. 0.8 mm) spinneret. Extrusion temperatures were varied between 145 °C and 220 °C depending on the blend composition.

Characterization of Alcell/PEO Blends. Tensile properties of Alcell and its PEO blend fibers were measured using an Instron Model 4411 with a 0.5 N Load Cell. The test speed was 0.5 mm min^{-1} and the sample length was 25 mm. Tensile tests were performed at constant temperature (25 °C) and relative humidity (65%). All reported results are the average of 20 tests.

Glass-transition temperatures, T_g, of the blends were determined on a TA Instruments Q 100 DSC at a scan rate of 20 °C/min over a temperature range of −90 to 200 °C. The measurements were made using 5.0−5.5 mg samples under a nitrogen atmosphere. The glass-transition temperature was recorded as the midpoint temperature of the heat capacity transition of the second heating run. Samples were run in duplicate and are reported as the average of the two runs and were within experimental error of each other (±1.0 °C).

The equilibrium melting point, T_m^{eq}, was determined by DSC using Hoffman-Weeks plots.[20] In a typical experiment, 5.0-mg samples were heated to 90 °C and held at temperature for 10 min to completely eliminate PEO crystallinity. The sample was than quenched to the desired isothermal crystallization temperature, T_{ic}, and held at temperature for 2 h to allow complete crystallization. After isothermal crystallization, the melting temperature, T'_m, was measured using a heating rate of 10 °C min^{-1}. T'_m was determined as the peak temperature.

Infrared (FT-IR) spectra of the polymer blends were determined using the diffuse reflectance (DRFT-IR) method. (Because of the physical properties of the polymer blends, it was difficult to prepare uniform KBr pellets for FT-IR analysis using transmittance detection.) The polymer blends (10 mg) were dispersed in KBr (200 mg) and DRFT-IR measurements were recorded on a Perkin-Elmer 16PG FT-IR spectrometer; 256 scans were collected with a spectral resolution of 4.0 cm^{-1}. Owing to the hygroscopic nature of the polymer blends, a pure nitrogen flow was maintained over the sample during collection.

X-ray diffraction (WAXD) analyses were performed at the Analytical Instrument Facility of North Carolina State University using a Norelco Diffractometer. X-ray diffractions were collected using nickel-filtered CuKα radiation (35 kV and 20 mA), 60 counts min^{-1} sampling rate, scanning a two-theta scan range of 10−35° at a scanning speed of 1° min^{-1}. No internal standard was used in these experiments.

Results and Discussion

Characterization of Alcell Lignin. The thermal properties of technical lignins vary depending on the species of wood and the chemical process utilized in its isolation. The presence of inorganic impurities, for example, ash, also reduces the thermal mobility of lignin molecules. For example, the glass-transition temperature, T_g, of lignin significantly increased and the thermal flow point, T_f, disappeared with the addition of small amounts of nickel acetate.[21] In technical lignins such as kraft lignins, the presence of ash is significant, such that the inorganic portions must be removed to enable satisfactory thermal processing.[14] The ash content of organosolv lignins is small because of the chemical process utilized, wherein the inorganic impurities are those which originated from the wood chips. The ash content for our Alcell lignin was <0.1% and the lignin exhibited good thermal processability. The T_g of the Alcell lignin was 70 °C. This is lower than that found for a commercial hardwood kraft lignin, T_g = 93 °C after ash removal. Thus, other factors such as chemical structure contribute to the thermal property of the Alcell lignin.

The effect of chemical structure on the thermal properties of lignins have been studied. Thermomechanical analysis of fractionated lignin revealed that both T_g and T_f increase with increasing lignin molecular weight.[3,22] However, the molecular weight of the Alcell lignin used in this study, MW = 2200 Da, is approximately the same as that determined previously for a hardwood kraft lignin, MW = 2400 Da (Table 1). Functional group and molecular weight analysis of the Alcell lignin are listed in Table 1, along with the results previously obtained for a hardwood kraft lignin.[4] The molar ratio of the syringyl, S, to guaiacyl, G, structures estimated by nitrobenzene oxidation is almost 2 times greater for the Alcell lignin than for the hardwood kraft lignin, 2.3 mmol g^{-1} versus 1.2 mmol g^{-1}, respectively, even though the methoxyl content of the respective

Table 1. Chemical Properties of Isolated Lignins

	functional groups (mmol g^{-1})					
	hydroxyl				molecular mass	
sample	aliphatic	aromatic	methoxyl	S G-1	MW	PDI
Alcell lignin	3.6	4.3	5.6	2.3	2200	1.7
hardwood kraft lignin	4.1	4.3	5.8	1.2	2400	1.9

lignins are approximately the same, 5.6 mmol g^{-1} versus 5.8 mmol g^{-1}. This implies that the Alcell lignin contains more condensed guaiacyl units than the hardwood kraft lignin.[16] However, a more condensed structure will reduce the thermal mobility of the lignin molecules. This seems to contradict the results obtained from thermal analysis. Further, it is well established that under the acidic conditions of the Alcell process, several carbonyl compounds, Hibbert's ketones, are produced from the acidic cleavage of aryl ether (β-O-4) bonds. In fact, FT-IR analysis of the Alcell lignin reveals a substantially higher carbonyl content as compared to the hardwood kraft lignin, Figure 1. These polar functional groups will participate in strong intermolecular interactions, such as hydrogen bonding, and further reduce the thermal mobility of the lignin molecules. Therefore, other structural features must affect the thermal properties of Alcell lignin and the observed relatively low T_g.

The chemical structure of technical lignins produced from the kraft process is dramatically different than that of organosolv. Under the alkaline conditions of kraft processing, side reactions, such as reverse aldol condensation reactions, occur wherein the γ-carbon is released as formaldehyde (Figure 2). In fact, kraft pulping of ^{14}C labeled lignin woodmeal revealed 45% of the C_γ carbon was eliminated during the 3h reaction.[23]

The γ-carbon is relatively stable toward acidolysis. Under acidic conditions, hydrolysis of benzyl ether linkages produce a resonance stabilized benzyl carbocation. This reactive intermediate will then undergo nucleophilic addition by the solvent, ethanol.[24] Thermal mobility of lignin is enhanced by the alkylation, esterification, and etherification.[25] Therefore, ethoxylation of the benzylic position along with retention of the propionoid side chain (more intact γ-positions) have potential to reduce T_g of the Alcell lignin relative to kraft lignin.

HMQC NMR spectra of the oxygenated aliphatic region for a hardwood kraft lignin (A) and the Alcell lignin (B) are shown in Figure 3. Included in the spectra are the assignments for (**1**) β-O-4 including the C_α- and C_γ-hydroxyl group assignments for syringyl (**S**) and guaiacyl (**G**) moieties, (**2**) pinoresinol ($\beta-\beta$), and (**3**) phenylcoumaran (β-5).[26] These spectra clearly demonstrate that the β-O-4 structures survive chemical processing and remain in both lignins.

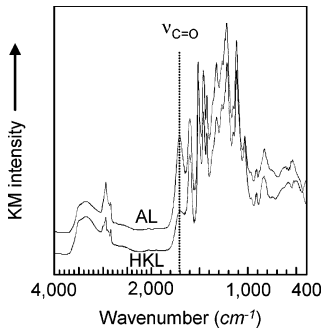

Figure 1. DRFT-IR spectra of Alcell lignin (AL) and hardwood kraft lignin (HKL).

Table 2. Mechanical Properties of Alcell/PEO Blend Fibers

Alcell/PEO ($w\ w^{-1}$)	tensile strength (MPa)	Young's modulus (MPa)	elongation (%)
100/0	18.7 ± 4.8	4570 ± 360	0.4 ± 0.1
95/5	22.6 ± 2.7	4090 ± 220	0.6 ± 0.1
87.5/12.5	19.2 ± 1.7	3270 ± 220	0.6 ± 0.1
75/25	5.9 ± 0.9	440 ± 30	3.1 ± 0.3
50/50	10.8 ± 1.4	750 ± 110	2.4 ± 0.4
25/75	10.2 ± 0.6	610 ± 60	44.8 ± 24.1
0/100	12.6 ± 0.2	510 ± 30	5.4 ± 0.6

The β-position in the β-O-4 lignin moieties, **1** ($\delta_H \sim 4.0-4.8/\delta_C \sim 80-86$), is more complex in the Alcell lignin than the hardwood kraft lignin. Ethoxylation of the benzylic position (structure **4** in Figure 3) shifts the β proton to lower magnetic field and the β carbon to higher magnetic field.[26] Accordingly, the chemical shift for the α-ethoxy-β-aryl ether moieties, **4**, are assigned **a** and **b** for the guaiacyl and syringyl units, respectively (Figure 3B).

Other distinct differences in the correlation peaks are observed, labeled I−IV in Figure 3. Unfortunately, all of these peaks cannot be accurately assigned. However, the cluster labeled III can be assigned as a correlation peak of γ-O-alkyl moieties (Figure 3B).[26] This functionalization of the lignin can arise through the acid-catalyzed reaction of ethanol (solvent) with the C_γ after dehydration of C_γ-hydroxyl group. Chain extension by this reaction would further enhance the thermal mobility of the lignin molecules through internal plasticization. Furthermore, becaue of the large variety of oxidation states of the β carbon in the Alcell lignin, new correlation peaks for the γ position appear around $\delta_H/\delta_C = 3.2-4.5/58-66$. Thus, the more intact propanoid side chain along with the α-O-alkyl (benzylic) and γ-O-alkyl moieties may contribute to the lower T_g of the Alcell lignin relative to the kraft lignin.

Preparation of Alcell/PEO Blend Fibers. Previously, it was found that the thermal processability of kraft lignin could be remarkably improved by the addition of PEO.[4] The effect of PEO blending on the thermal spinning temperatures of various Alcell/PEO blends are shown in Figure 4. All blends exhibited good thermal processing properties with continuous fibers being spun for more than 30 min at ca. 100 m min^{-1} (the maximum winding rate of our take-up device). (Interestingly, some of the Alcell rich fibers, 87.5−50 wt %, adhered to each other on the spool core during the take-up process.) Spinning temperatures decreased with increasing addition of PEO, the lowest temperature observed for Alcell/PEO 50/50 blend consistent with the hardwood kraft lignin/PEO system.[4] This coplasticizing effect indicates a change in the physical properties of the blend or its components, such as interchain interactions upon changing blend composition.

Mechanical properties of the Alcell/PEO blends are shown in Figure 5 and summarized in Table 2. The Young's modulus (4.6 GPa) and tensile strength (18.7 MPa) of the Alcell lignin are comparable to reported values for other organosolv[27] and hardwood kraft lignins.[4]

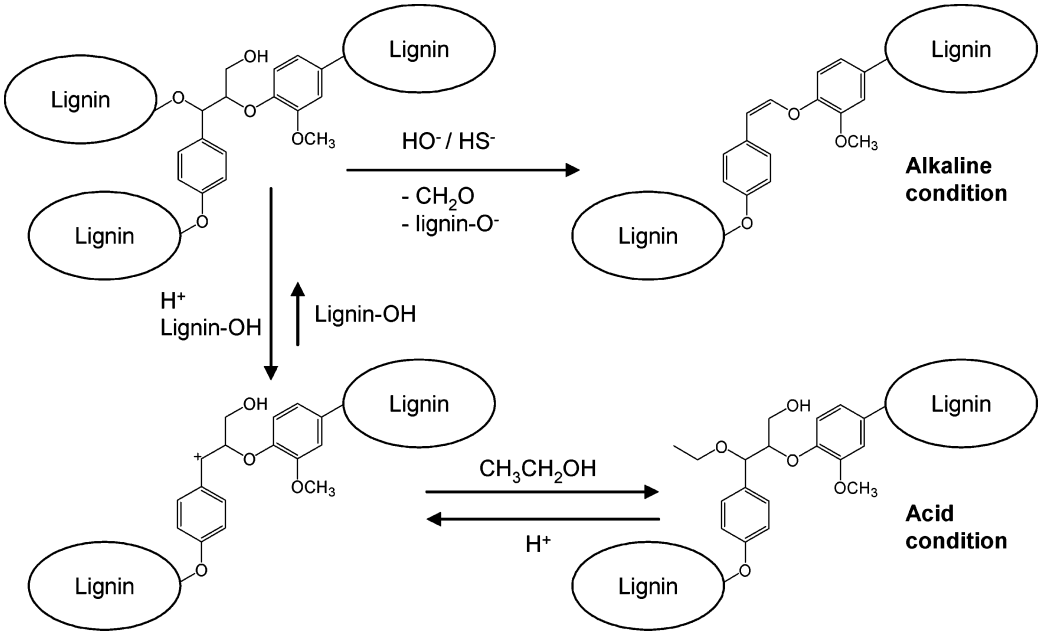

Figure 2. Expected reaction on benzyl position during lignin isolation process.

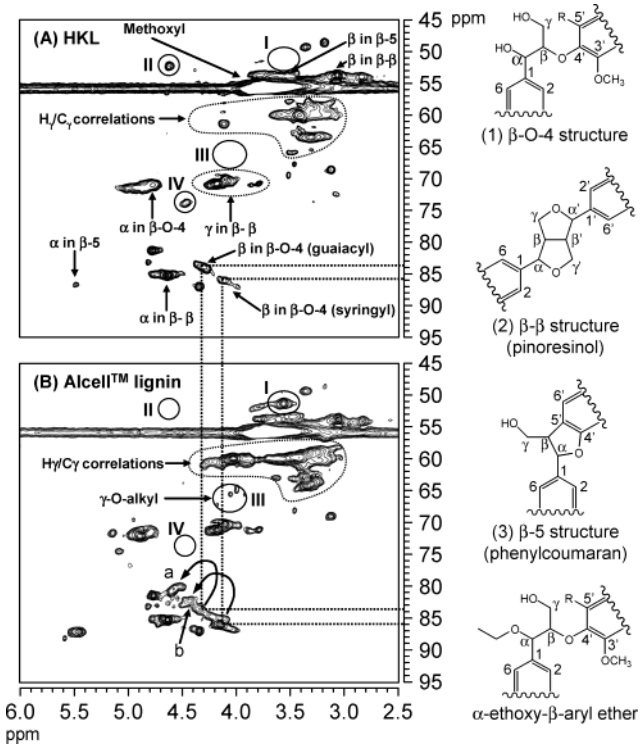

Figure 3. HMQC spectra of oxygenated aliphatic region of HKL (A) and Alcell lignin (B).

Low wt % additions of PEO affect both the Young's modulus and tensile strength. Incorporation of 5 wt % of PEO decreased the Young's modulus, while it increased the tensile strength. Increasing addition of PEO dramatically reduced both the Young's modulus and tensile strength of the Alcell lignin-based fibers, reaching a minimum at 25 wt % PEO incorporation. The initial increase in tensile behavior is likely the result of PEO disrupting the noncovalent attractive interactions of the lignin macromolecules.[3] Increasing PEO incorporation further disrupts the supramacromolecular lignin structure and the observed physical properties become more strongly influenced by the PEO component. This is consistent with a miscible polymer blend

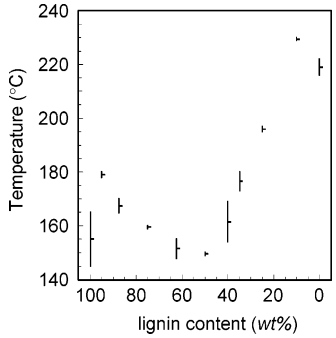

Figure 4. Relation ships between spinning temperature and blend composition of lignin.

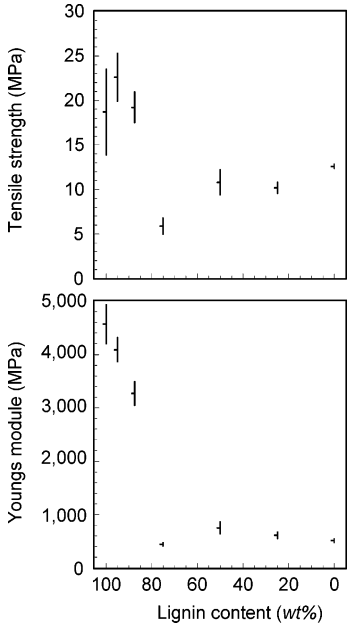

Figure 5. Tensile strength and Young's modulus of Alcell lignin/PEO fibers as a function of lignin content.

system. Notable is the difference in the rate of change in tensile behavior between the Alcell lignin/PEO blends and the hardwood kraft lignin/PEO blends. In the

Table 3. DSC Results of the AlcellTM Lignin/PEO Blend Fibers

weight fraction ($w\ w^{-1}$)						weight fraction in amorphous phase ($w\ w^{-1}$)	
lignin	PEO	T_g (°C)	ΔC_p (J g^{-1} °C^{-1})	T_m (°C)	ΔH (J g^{-1})	lignin	PEO
1.00	0.00	80	0.69	×	0	1.00	0.00
0.95	0.05	76	0.74	×	0	0.95	0.05
0.87	0.13	49	0.72	×	0	0.87	0.13
0.75	0.25	25	0.74	×	0	0.75	0.25
0.62	0.38	−3	0.75	×	0	0.62	0.38
0.50	0.50	−22	0.82	53[a]	6[a]	×[a]	×[a]
0.40	0.60	−37	0.24	53	68[a]	×[a]	×[a]
0.35	0.65	−2	0.36	56	75	0.60	0.40
0.25	0.75	−4	0.30	60	111	0.64	0.36
0.10	0.90	−31	0.28	63	150	0.49	0.51
0.00	1.00	−50	0.12	67	168	0.00	1.00

[a] There was some difficulty in the determination of these values by DSC because of the recrystallization peak.

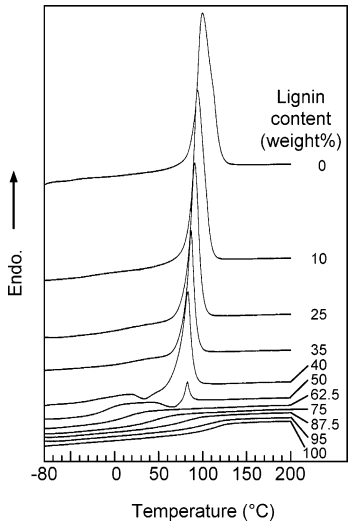

Figure 6. DSC curves of Alcell lignin/PEO blend fibers.

hardwood kraft lignin system, after an initial increase the tensile strength decreased gradually to a minimum at 100% PEO. This apparent difference may be the result of differences in the magnitude and extent of lignin intermolecular association in Alcell lignin as compared to kraft lignins. This phenomenon is currently being investigated.

Melting and Crystallization Behavior of Alcell Lignin/PEO Blends. The results of differential scanning calorimetric (DSC) analysis of Alcell lignin/PEO blends of various compositions are shown in Figure 6 and summarized in Table 3. The melting temperature, T_m, of the PEO fraction in the blends decreased with increasing Alcell lignin content. Similarly, the crystallinity of the PEO fraction dramatically decreased with increasing Alcell lignin content, with no T_m detected in blends with Alcell lignin content beyond 62.5 wt %, Table 4. This crystalline behavior suggests that the PEO is completely dispersed within the Alcell lignin.

The WAXD patterns of the Alcell lignin/PEO blends are shown in Figure 7. Typical reflections are observed at $2\theta = 19.1°$ and 23.4°, assigned to 120 and 112/004 planes, respectively.[28] The 120 plane is parallel to the molecular axis while 112/004 plane is more orthogonal to the molecular chain direction. It is clear that the peak positions from the WAXD profiles of the various Alcell lignin/PEO blends are almost identical. This indicates that the unit-cell dimensions of PEO are not disturbed by blending with Alcell lignin. Interestingly, the relative intensity of the peak at 23.4−19.1° decreases with

Table 4. Results Obtained from the Hoffman-Weeks Plot

weight fraction ($w\ w^{-1}$)		relative		stability
lignin	PEO	crystallinity[b]	T_m^0 (°C)	parameter, ϕ
0.50	0.50	0.07[a]		
0.40	0.60	0.67[a]	59.2	0.194
0.35	0.65	0.71	59.8	0.178
0.25	0.75	0.91	62.3	0.116
0.10	0.90	0.99	65.8	0.094
0.00	1.00	1.00	68.9	0.129

[a] There was some difficulty in determining these values because of the recrystallization peak (see Figure 5). [b] The relative crystallinity was calculated from the heat of fusion values from the DSC curves.

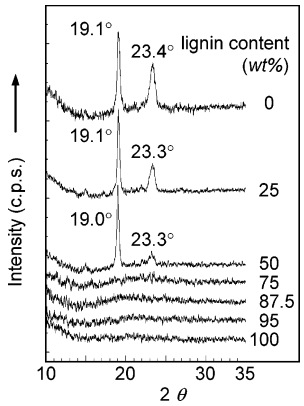

Figure 7. WAXD patterns of the Alcell lignin/PEO blend fibers.

increasing Alcell lignin content. This suggests that the ordered structure between PEO molecular chains is affected more than that for the chain direction by blending with Alcell lignin. Finally, both reflections completely disappear at blend ratios of more than 50 wt % Alcell lignin.

Crystalline size and perfection of PEO can be estimated from the Hoffman-Weeks plot shown in Figure 8. This plot is based on $T_m^0 - T_m = \phi(T_m^0 - T_c)$, where T_m and T_m^0 are the observed and equilibrium melting temperature respectively, T_c is isothermal crystallization temperature, and ϕ is the stability parameter.[29] Good linearity is observed between T_c and T_m for the Hoffman-Weeks plot of the Alcell lignin/PEO. Extrapolation of the data for the PEO homofiber determined T_m^0 to be ∼68.9 °C (Table 4). This T_m^0 value is in good agreement with reported values.[30] For stable large crystals $T_m = T_m^0$ and ϕ equals zero, whereas ϕ approaches 1 in an unstable crystal.[31] Therefore, ϕ is the reciprocal to crystalline size and perfection. As listed in Table 4, the ϕ value of the PEO decreased by blending

Table 5. Parameters Estimated from T_g Variation Curves of Alcell Lignin/PEO Blends

	equation[a]	parameter
Fox:	$\frac{1}{T_g} = \frac{w_1}{T_{g1}} + \frac{w_2}{T_{g2}}$	($R^2 = 0.866$)
Couchman:	$\ln T_g = \frac{w_1 \Delta C_{p1} \ln T_{g1} + w_2 \Delta C_{p2} \ln T_{g2}}{w_1 \Delta C_{p1} + w_2 \Delta C_{p2}}$	($R^2 = 0.827$)
Gordon-Taylor:	$T_g = \frac{w_1 T_{g1} + k w_2 T_{g2}}{w_1 + k w_2}$	$k = 0.37 \pm 0.04$ ($R^2 = 971$)
Kwei:	$T_g = \frac{w_1 T_{g1} + k w_2 T_{g2}}{w_1 + k w_2} + q w_1 w_2$	$q = -147 \pm 10$, $k = 1$ ($R^2 = 0.987$)

[a] T_g, T_{g1}, and T_{g2} are the glass-transition temperature of the blend and homopolymers, respectively. w_1 and w_2 are the corresponding weight fractions. ΔC_{p1} and ΔC_{p2} are the magnitude of increase in heat capacity at the T_g of corresponding homopolymers.

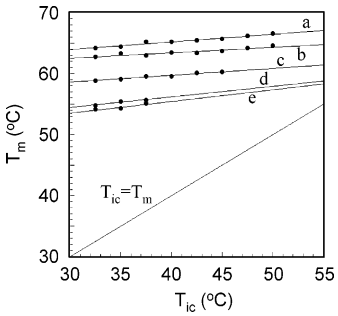

Figure 8. Hoffman-Weeks plot for Alcell lignin/PEO blends a, 0/100; b, 10/90; c, 25/75; d, 35/65; e, 40/60.

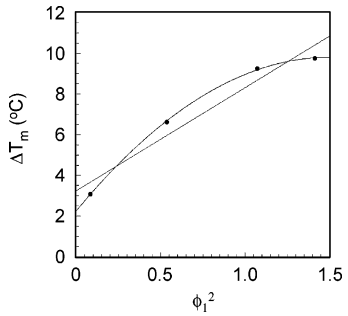

Figure 9. Melting point depression of PEO fraction in Alcell/PEO blends.

with small amounts of Alcell lignin, which indicates that Alcell lignin increases the crystalline size of PEO. The crystallization behavior of PEO has been reported to be impacted by strong interacting polymer blend systems.[32] Thus, Alcell lignin may enhance the flexibility of the PEO molecules and subsequent crystallization. This is in agreement with the spinning temperature results shown in Figure 3. The spinning temperature of PEO, which may be related to molten viscosity, decreases upon blending with Alcell lignin; however, ϕ increased with lignin incorporation beyond 25 wt %. This suggests that the PEO crystalline size or perfection and crystallinity decreased with increased Alcell lignin content. Such a change in ϕ values is not observed in softwood kraft lignin/PEO blends. The ϕ value of softwood kraft lignin/PEO blends is stable, $\phi = 0.118-0.129$ (unpublished results). It could be said that Alcell lignin may favorably mix with PEO more than with softwood kraft lignin. Perhaps during PEO crystallization, the Alcell lignin molecules interact with the interlamella region thereby affecting the crystalline growth more in the parallel direction than in the orthogonal direction. This may be related to the observed imperfection of the 112/004 plane as described in the WAXD section.

The Hoffman-Weeks approach estimates a large T_m^0 depression for the Alcell lignin/PEO blend fibers, 9.8 °C for the 40/60 blend. The T_m^0 depression plot is not linear, implying a composition dependent interaction parameter (Figure 8).[33,34] Such nonlinearity was also observed for the softwood kraft lignin/PEO blends (data not shown). Using the Nishi-Wang equation, an interaction energy density value, $B = -7.7$, was calculated for the Alcell lignin/PEO blends.[35] This value is higher than that determined for other lignin/PEO blend systems, -5.5 and -4.8 for hardwood[4] and softwood kraft lignin/PEO blend systems, respectively. Thus, the intermolecular interactions between PEO and Alcell lignin are greater than with other lignins.

Glass-Transition Behavior of Alcell Lignin/PEO Blend Fibers. Further information can be estimated from the glass-transition temperature (T_g) behavior of the polymer blends. The Alcell lignin/PEO blend fibers show a single compositional dependent T_g over the entire blend ratio, which decreases with increasing PEO content (Figure 9). The single compositional-dependent T_g is an indication of full miscibility on a dimensional scale between 5 and 15 nm.[36] Figure 9 demonstrates that the T_g exhibits a negative deviation from the linear additive indicative of relatively weak favorable interactions between components.[37] Several theoretical and empirical equations have been proposed for the prediction of T_g in miscible polymer blends, on the basis of the composition of the blend, the T_g's of the individual components, and the nature of the interactions between these components.[37−40] Table 5 lists several of these equations along with the respective parameters determined from the observed Alcell lignin/PEO blend T_g behavior. Among these, the Gordon-Taylor[38] and Kwei[39] equations provide an adequate fit of the experimental data (Figure 9). The calculated fitting parameters in the Gordon-Taylor, k, and Kwei, q, equations indicate the quality and quantity of intermolecular interactions between blend components, respectively. From the experimental data plotted in Figure 9, $k = 0.37$ and $q = -147$ for the Alcell lignin/PEO blend system. Compared with hardwood kraft where $k = 0.37$ and $q = -170$ and softwood kraft/PEO blends where $k = 0.27$ and $q = -269$, the values obtained for the Alcell lignin reveal the presence of stronger intermolecular interactions (larger k) and a higher propensity to form intermolecular interactions (less negative q). The observed T_g behavior of the Alcell lignin/PEO blends are in agreement with the interaction energy density value B calculated from T_m^0 depression.

Hydrogen Bonding in the Alcell Lignin/PEO Blend Fibers. One of the most effective means to

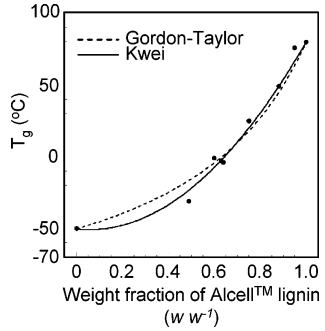

Figure 10. Composition dependence on T_g of Alcell lignin/PEO blends.

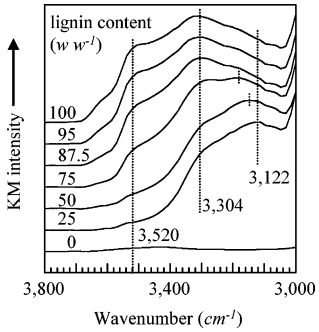

Figure 11. DRFT-IR spectra of Alcell lignin/PEO blend fiber in the $\nu_{(O-H)}$ region.

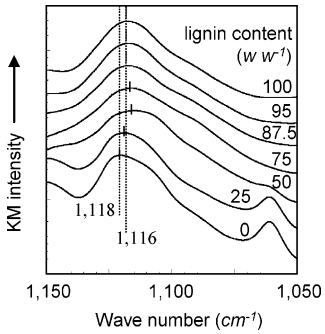

Figure 12. DRFT-IR spectra of Alcell lignin/PEO blend fiber in the $\nu_{(C-O-C)asym}$ region.

investigate specific intermolecular interactions between polymers is FT-IR spectroscopy. FT-IR can be used qualitatively and quantitatively to estimate hydrogen-bonding interactions between blend components. Figure 10 shows the FT-IR spectra of the hydroxyl stretching (ν_{OH}) region (3000−3800 cm^{-1}) of Alcell lignin in the respective PEO blends. The Alcell lignin homofiber shows a broad band at ∼3304 cm^{-1} and a shoulder at ∼3520 cm^{-1}. From the FT-IR analysis of lignin model compounds,[4] the shoulder at ∼3520 cm^{-1} can be assigned to intramolecular hydrogen bonding in aromatic hydroxyl groups or intermolecular (dimer) hydrogen bonding between lignin molecules. The broad band at 3304 cm^{-1} can be assigned to multiple intramolecular hydrogen bonding. In the kraft lignin homofibers, the ν_{OH} band center (∼3422 cm^{-1}) appears at a higher wavenumber region than that of the Alcell lignin homofiber (∼3304 cm^{-1})[4] indicating stronger hydrogen bonding in the Alcell lignin as compared to the kraft lignin. The Alcell lignin contains a significant amount of carbonyl groups that can form strong hydrogen bonds with hydroxyl group. Therefore, the lower wavenumber for the broad ν_{OH} band of the Alcell lignin homofiber could be due to strong hydrogen bonding with the carbonyl groups.

Blending with PEO dramatically changes the ν_{OH} region of the FT-IR spectra, indicative of changes in the hydrogen-bonding systems. The relative band intensities of the ∼3520 cm^{-1} shoulder and ∼3304 cm^{-1} broad band observed in the Alcell lignin homofiber decrease with the blending of PEO, while a third band appears between 3100 and 3200 cm^{-1}. Increasing PEO content leads to further intensity reduction of the higher wavenumber bands (∼3520 and ∼3304 cm^{-1}) and an increase in the intensity of the lower wavenumber band (∼3100 cm^{-1}). Similarly, the carbonyl stretching band ($\nu_{C=O}$) at ∼1709 cm^{-1} decreases in intensity with increasing PEO content but does not indicate a wavenumber shift (data not shown). This implies that the existing hydrogen bonds are either very strong and not disrupted upon blending with PEO, just the relative intensity decreases because of dilution with PEO, or that the extent of change in wavenumber is too small to be detected at the resolution of our studies. At 75 wt % PEO, the broad band at ∼3304 cm^{-1} and the shoulder at ∼3520 cm^{-1} are almost completely gone and a primary band is observed at ∼ 3122 cm^{-1}. Thus, the majority of intramolecular or intermolecular hydrogen bonding within and between the lignin are replaced with stronger intermolecular hydrogen bonds with PEO.

A corresponding effect is observed in the asymmetric C−O−C stretching ($\nu_{asC-O-C}$) region (1050−1150 cm^{-1}) of these blends. In the Alcell lignin and PEO homofibers, these bands appear at 1118 cm^{-1} and 1116 cm^{-1}, respectively. However, the $\nu_{asC-O-C}$ band of PEO shifts to a lower wavenumber region when blended with Alcell lignin as shown in Figure 12. This is consistent with the observed effect in the ν_{O-H} region. This supports the idea that new specific hydrogen-bonding interactions are formed between the ether group of the PEO and the hydroxyl groups of the lignin upon thermal blending of PEO with Alcell lignin.

Summary

Organosolv lignin, Alcell, was thermally blended with PEO over a range of blend compositions. Compared with kraft lignins, Alcell lignin displayed better plastic behavior and the corresponding PEO blends possessed excellent thermoforming properties. Continuous fiber spinning was readily achieved by fusion spinning. The excellent thermal properties arise because of the chemical structure of the Alcell lignin. HMQC 2D NMR analysis of the Alcell lignin revealed flexible alkoxyl chains are introduced at the Cα and Cγ positions of lignin side chain structure during the isolation process from wood. These moieties act as internal plasticizers enhancing the thermal mobility of the lignin.

Miscible blends were observed over the entire blend ratio. The addition of a small amount of Alcell lignin to PEO resulted in an increase of the PEO crystalline domain size. However, both PEO crystallinity and crystalline domain size decreased with lignin incorporation beyond 25 wt %. On the basis of WAXD analysis, it is postulated that Alcell lignin may hinder crystallization in the 120 direction more than in the 112/004 direction.

A weak favorable interaction between blend components was determined on the basis of T_g behavior. Analysis using the Gordon-Taylor and Kwei equations revealed that the Alcell lignin/PEO blended exhibit stronger intermolecular interactions and a higher pro-

pensity to form them than in other lignin/PEO blend systems. This result is in good agreement with the interaction energy density values, *B*, calculated from equilibrium melting point depression. FT-IR analysis revealed the formation of a strong hydrogen-bonding system between Alcell lignin and PEO, further supporting the idea that hydrogen-bonding interactions may be an important factor in the formation of miscible lignin-based polymer blends.

Acknowledgment. Financial support from USDA-IFAFS (Grant # 2001-52104-11224) is gratefully acknowledged. The authors would also like to thank R. D. Gilbert and H.-m. Chang for their helpful discussion of the manuscript.

References and Notes

(1) Hu, T. Q. *Chemical modification, properties, and usage of lignin*; Kluwer Academic/Plenum Publishers: New York, 2002.
(2) Tudorachi, N.; Cascaval, C. N.; Rusu, M. *J. Polym. Eng.* **2000**, *20*, 287−304.
(3) Li, Y.; Sarkanen, S. *Macromolecules* **2002**, *35*, 9707−9715.
(4) Kadla, J. F.; Kubo, S. *Macromolecules* **2003**, *36*, 7803−7811.
(5) Kadla, J. F.; Kubo, S. *Composites, Part A: Applied Science and Manufacturing* **2004**, *35*, 395−400.
(6) Kubo, S.; Kadla, J. F. *Biomacromolecules* **2003**, *4*, 561−567.
(7) Li, Y.; Mlynar, J.; Sarkanen, S. *J. Polym. Sci., Part B: Polym. Phys.* **1997**, *35*, 1899−1910.
(8) Glasser, W. G.; Sarkanen, S. *Lignin: properties and materials*, 1989.
(9) Higuchi, T. *Biosynthesis and biodegradation of wood components*; Academic Press: Orlando, FL, 1985.
(10) Sederoff, R. R.; Chang, H.-m. In *Wood structure and composition*; Lewin, M., Goldstein, I. S., Eds.; M. Dekker: New York, 1991; pp xiv, 488.
(11) Terashima, N.; Fukushima, K.; He, L.-F.; Takabe, K. *Forage cell wall structure and digestibility*; American Society of Agronomy Inc.: Madison, WI, 1993.
(12) Sarkanen, S.; Teller, D. C.; Stevens, C. R.; McCarthy, J. L. *Macromolecules* **1984**, *17*, 2588−2597.
(13) Sarkanen, S.; Teller, D. C.; Hall, J.; McCarthy, J. L. *Macromolecules* **1981**, *14*, 426−434.
(14) Kadla, J. F.; Kubo, S.; Venditti, R. A.; Gilbert, R. D.; Compere, A. L.; Griffith, W. *Carbon* **2002**, *40*, 2913−2920.
(15) Feldman, D.; Banu, D. *J. Appl. Polym. Sci.* **1997**, *66*, 1731−1744.
(16) Liu, Y.; Carriero, S.; Pye, K.; Argyropoulos, D. S. In *Lignin: Historical, Biological, and Materials Perspectives*; American Chemical Society: Washington, DC, 2000; Vol. 742, pp 447−464.
(17) Chen, C.-L. In *Springer series in wood science*; Dence, C. W., Ed.; Springer-Verlag: New York, 1992; pp 301−321.
(18) Chen, C.-L. In *Methods in lignin chemistry*; Lin, S. Y., Dence, C. W., Eds.; Springer-Verlag: New York, 1992; pp 301−321.
(19) Shimatani, K.; Sano, Y.; Sasaya, T. *Holzforschung* **1994**, *48*, 337−342.
(20) Hoffman, J. D.; Weeks, J. J. *J. Chem. Phys.* **1962**, *37*, 1723−&.
(21) Kubo, S.; Uraki, Y.; Sano, Y. *J. Wood Sci.* **2003**, *49*, 188−192.
(22) Kubo, S.; Uraki, Y.; Sano, Y. *Holzforschung* **1996**, *50*, 144−150.
(23) Araki, H.; Tomimura, Y.; Terashima, N. *Mokuzai Gakkaishi* **1977**, *23*, 378−382.
(24) McDonough, T. J. *Tappi J.* **1993**, *76*, 186−193.
(25) Lewis, H. F.; Brauns, F. E.; Buchanan, M. A.; Brookbank, E. B. *Ind. Eng. Chem.* **1943**, *35*, 1113−1117.
(26) Capanema, E. A.; Balakshin, M. Y.; Kadla, J. F. *J. Agric. Food Chem.* **2004**, *52*, 1850−1860.
(27) Uraki, Y.; Kubo, S.; Nigo, N.; Sano, Y.; Sasaya, T. *Holzforschung* **1995**, *49*, 343−350.
(28) Huang, C. I.; Chen, J. R. *J. Polym. Sci., Part B: Polym. Phys.* **2001**, *39*, 2705−2715.
(29) Hoffman, J. D.; Weeks, J. J. *J. Chem. Phys.* **1962**, *37*, 1723−1729.
(30) Pedrosa, P.; Pomposo, J. A.; Calahorra, E.; Cortazar, M. *Polymer* **1995**, *36*, 3889−3897.
(31) Hoffman, J. D.; Miller, R. L. *Polymer* **1997**, *38*, 3151−3212.
(32) Talibuddin, S.; Wu, L.; Runt, J.; Lin, J. S. *Macromolecules* **1996**, *29*, 7527−7535.
(33) Cheung, Y. W.; Stein, R. S. *Macromolecules* **1994**, *27*, 2512−2519.
(34) Painter, P. C.; Tang, W. L.; Graf, J. F.; Thomson, B.; Coleman, M. M. *Macromolecules* **1991**, *24*, 3929−3936.
(35) Nishi, T.; Wang, T. T.; Kwei, T. K. *Macromolecules* **1975**, *8*, 227−234.
(36) Paul, D. R.; Bucknall, C. B. *Polymer blends*; Wiley: New York, 2000.
(37) Lu, X.; Weiss, R. A. *Macromolecules* **1992**, *25*, 3242−3246.
(38) Gordon, M.; Taylor, J. S. *J. Appl. Chem.* **1952**, *2*, 493−500.
(39) Kwei, T. K.; Pearce, E. M.; Pennacchia, J. R.; Charton, M. *Macromolecules* **1987**, *20*, 1174−1176.
(40) Couchman, P. R. *Macromolecules* **1978**, *11*, 1156−1161.

MA0490552